

Cooling and exhumation of the Trans-Himalayan Ladakh batholith as constrained by fission track apatite and zircon ages

Rajeev Kumar¹, Nand Lal², Sandeep Singh^{1,*} and A. K. Jain¹

¹Department of Earth Sciences, Indian Institute of Technology Roorkee, Roorkee 247 667, India

²Department of Geophysics, Kurukshetra University, Kurukshetra 136 119, India

Low-temperature thermochronology of the Trans-Himalayan Ladakh batholith has been applied, using fission track (FT) dating of apatite and zircon separates, to work out the exhumation history. Thirty FT apatite samples from the Ladakh Batholith provide an excellent constraint on its exhumation at low temperature ~ 110°C. The oldest apatite ages of 23.1 ± 1.1 Ma from the Khardung La (5440 m) and 25.4 ± 2.6 Ma from the Chang La (5301 m) have been obtained from the highest uplifted parts of the batholith, while the youngest ages are 11.8 ± 1.1 Ma (4038 m) and 9.2 ± 0.9 Ma (3732 m) respectively. Apatite ages from Lyoma-Hanle section are tightly clustered between 17.8 and 12.0 Ma. Elevation profiles of these two sections yield exhumation rates of 0.1 mm/a for the Khardung La and Chang La sections between 25 and 9 Ma. In addition, three cogenetic zircons yielded FT ages of 41.4 ± 2.3 , 43.8 ± 3.4 and 31.7 ± 2.7 Ma, indicating a younging of the FT age from west to east. These FT data from the batholith indicate a slow cooling and exhumation history, as inferred from elevation vs age FT apatite plots.

Keywords: Exhumation, fission track dating, Ladakh Batholith.

THE Himalayan orogeny, the youngest in the history of the earth, has drawn global attention of geoscientists as the Himalayan mountains manifest the present and past records of collision tectonics. In recent years, one aspect of the Himalaya that has particularly drawn much attention is its cooling, exhumation and denudation history. For this purpose, thermochronology is widely applied to provide time and temperature coordinates in determining the cooling and exhumation rates. The potential of fission track (FT) zircon and apatite clocks is to provide time data for low-temperature history of a rock, and has promoted its widespread usage in many active mountain belts such as the Rockies¹, the Andes², the Transantarctic mountains³ and the Alps⁴. This technique has also been applied in the Indian sector of the Himalaya⁵⁻¹³ to unravel the cooling and exhumation patterns of the Himalayan metamorphic

belt and other tectonic units. In contrast, the Trans-Himalayan tectonic units, including the Ladakh batholith have been poorly constrained as far as their cooling and exhumation patterns are concerned. Though some cooling ages of FT zircon, apatite, K–Ar biotite and hornblende have been reported from different sectors of the batholith^{6,12}, age data are scarce and scattered. Here, we investigate the low temperature thermochronology using FT apatite and zircon ages in understanding the thermal and exhumation history of the Trans-Himalayan Ladakh batholith.

Geological framework

The junction between the Indian and Eurasian plates during the Late Mesozoic is defined by almost continuous Indus Tsangpo Suture Zone (ITSZ) and encompasses various lithologies like dismembered ophiolite mélanges at Nidar, Shergol and Zildat to name a few, within the Indus flysch sediments. These represent the part of the Neo-Tethys oceanic crust and trench, and its overthrust Spongtong klippe to the south. Within the suture zone, an Upper Jurassic to Upper Cretaceous Dras Volcanic island arc mainly of basalt, dacite, pillow lavas, and chert is developed in the western parts. Also, one finds subsequent fluvial clastics of the Indus molasse, which are mainly derived from the eroded adjoining provenances¹⁴⁻¹⁶.

The Trans-Himalayan batholiths, lying immediately to the north of the ITSZ for almost the entire length of the Himalaya, represent an Andean-type calc-alkaline magmatism due to subduction of the Neo-Tethyan oceanic crust under the Eurasian Plate during early Cretaceous–Lower Eocene^{17,18} (Figure 1a). The Trans-Himalayan batholith is variously known as the Kohistan batholith in Pakistan, the Ladakh batholith in India, Kailash and Gangdese plutonic complex in South Tibet and Lohit batholith in Arunachal Pradesh. About 3 km of the exposed thickness of the Ladakh batholith constitutes an important feature of this belt, which is about 600 km long and 30–80 km wide (Figure 1b). It extends from Astor, Deosai and Skardu in the northwest through Leh, Upshi, Lyoma to Demchuk and further southeast into southern Tibet^{16,18}. It is predominantly biotite- and hornblende-bearing granodiorite with minor occurrences of noritic gabbro, diorite and gran-

*For correspondence. (e-mail: sandpfes@iitr.ernet.in)

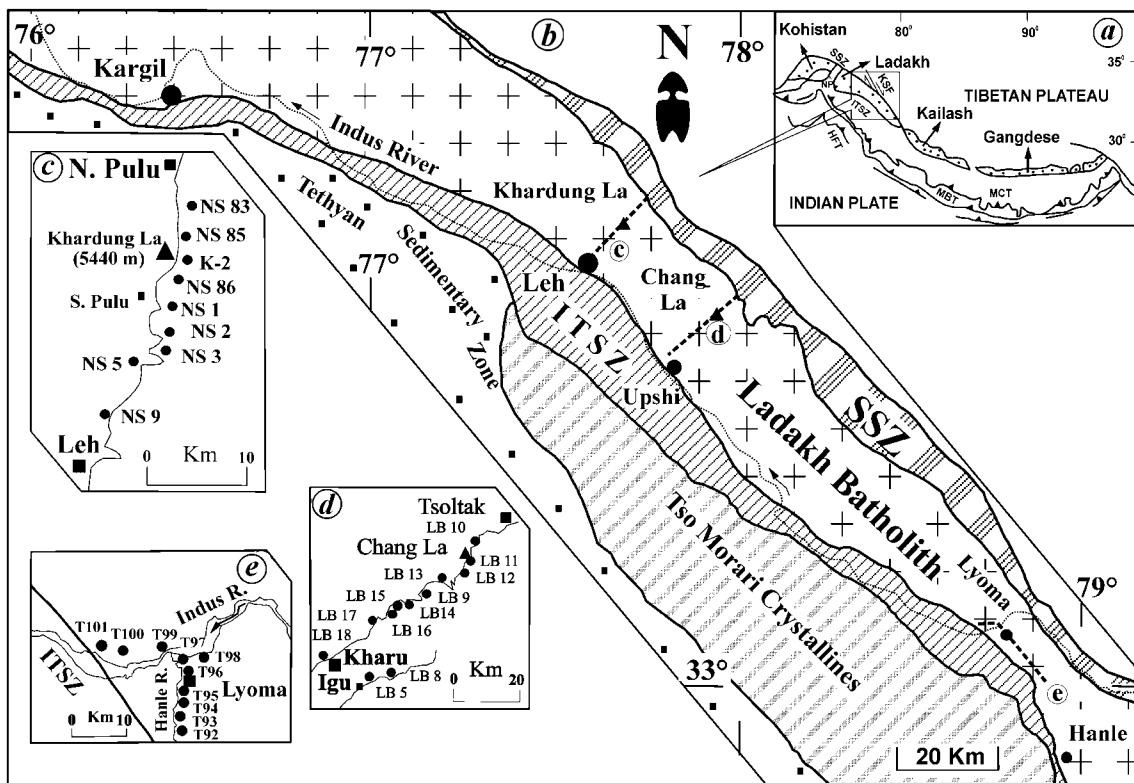


Figure 1. Simplified geological map of the Trans-Himalayan tectonic units, including the Ladakh Batholith. *a*, Location of Andean-type Trans-Himalayan batholiths. *b*, Geological setting of the Ladakh batholith in parts of Kargil–Leh–Hanle sector. ITSZ, Indus Tsangpo Suture Zone and SSZ, Shyok Suture Zone. Location of fission track samples used in this study from *c*, Leh–Khardung La section, *d*, Kharu–Chang La section and *e*, Lyoma–Hanle section. (Map modified after Thakur¹⁶ and our own observations.)

ite. It is distinctly an I-type cordilleran granitoid and appears to have been emplaced between 100 and 40 Ma with a dominant phase around 60 Ma¹⁵. A large sliver of sedimentary sequence within the Ladakh batholith suggests that it may have developed in a transitional environment between the Kohistan–Dras island arc in the west and the continental margin of Eurasia¹⁹.

The northern boundary of the Ladakh batholith is demarcated by another suture zone – the Shyok Suture Zone (SSZ) or Main Karakoram Thrust (MKT in Pakistan) having dismembered tectonic mélanges of ultramafics, gabbro, basalt and sediments. It demarcates the southern margin of the Karakoram Batholith Complex (KBC), which intrudes the Paleozoic–Mesozoic platform sediments of the Eurasian Plate. The SSZ extends to the NW beyond the Nanga Parbat spur and terminates against the ITSZ in Tibet. The SSZ has been grouped as the northern part of the Kohistan–Ladakh Arc and is reactivated into a steep MKT²⁰.

Sample preparation and analytical procedure

Thirty selected samples of diorite, granodiorite and granite from three most accessible sections of the Ladakh batholith in the southeast were prepared for FT analysis using

conventional crushing, sieving, magnetic and heavy-liquid separations to recover apatite and zircon fractions. These sections include Leh–Khardung La (9 samples), Kharu–Chang La (11 samples) and Lyoma–Hanle sections (10 samples) (Figure 1 *c–e*). Hand-picked apatite grains were mounted in Araldite at room temperature, and zircon grains on PFA Teflon at 320°C. Subsequently, grinding, polishing, etching, irradiation with thermal neutrons and counting of spontaneous and induced tracks in uranium-free Brazilian muscovite detector were carried out under 1500x magnification using 100x dry objective for calculating the FT ages^{11,21,22}. Fission track FT ages have been determined by the External Detector Method and calculated using the zeta calibration^{23,24}, according to IUGS Subcommittee on Geochronology by the Fission Track Working Group²⁵. The zeta value for apatite and zircon is 296.96 ± 8.18 in this study (D. Kumar, unpublished).

Results

FT ages

The FT analytical data of apatite and zircon samples are presented in the Tables 1 and 2. FT apatite ages range

Table 1. Apatite fission track data of Ladakh batholith

Sample code	Lab code	Elevation (m)	No. of crystals	Track density		$P(\chi^2)$ (%)	Glass dosimeter $\rho_d(N_d)$	Age (Ma)
				Spontaneous $\rho_s(N_s)$	Induced $\rho_i(N_i)$			
Leh–Khardung La section								
NS 1/1	KA1	4645	52	0.3605 (451)	3.3173 (4150)	85	0.7777 (3111)	12.5 ± 0.7
NS 2/3	KA2	4600	47	0.3406 (345)	2.0583 (2085)	30	0.7777 (3111)	19.1 ± 1.2
NS 3/7	KA3	4427	54	0.4225 (545)	3.4721 (4479)	80	0.7777 (3111)	14.0 ± 0.7
NS 5/12	KA4	4401	24	0.4500 (288)	3.4484 (2207)	30	0.7777 (3111)	15.1 ± 1.0
NS 9/20	KA5	4038	39	0.2989 (284)	2.9253 (2779)	80	0.7777 (3111)	11.8 ± 0.8
K-2	KA6	5440	50	0.5837 (610)	2.9167 (3048)	70	0.7777 (3111)	23.1 ± 1.1
NS83/157	KA7	5071	41	0.3854 (451)	2.2701 (2656)	90	0.7777 (3111)	19.6 ± 1.1
NS 5/162	KA9	5375	17	0.3312 (156)	1.7303 (815)	10	0.7777 (3111)	22.7 ± 2.0
NS86/163	KA10	5305	26	0.5241 (294)	2.9340 (1646)	<10	0.7777 (3111)	20.6 ± 1.4
Kharu–Chang La section								
LB 8/23	8/23A	3572	18	0.5225 (209)	3.885 (1554)	70	0.5025 (2010)	10.0 ± 0.8
LB 9/27	AP4	4572	15	0.6000 (219)	3.1096 (1135)	80	0.5025 (2010)	14.4 ± 1.1
LB 10/28	AP22	5301	7	0.8915 (115)	5.6279 (726)	80	1.0800 (4320)	25.4 ± 2.6
LB 11/29	11/29A	5060	23	0.5391 (252)	3.0102 (1463)	20	0.7777 (3111)	20.1 ± 1.4
LB 12/30	12/30A	4893	23	0.5391 (262)	2.8786 (1399)	90	0.7777 (3111)	21.6 ± 1.5
LB 13/31	AP14	4742	9	0.4933 (111)	2.1467 (483)	> 95	0.5025 (2010)	17.1 ± 1.8
LB 14/32	14/32A	4409	31	0.6227 (449)	6.3925 (4609)	80	1.0800 (4320)	15.6 ± 0.8
LB 15/33	AP11	4241	28	0.5039 (325)	5.6356 (3635)	30	0.9867 (3947)	13.1 ± 0.8
LB 16/34	16/34A	4072	21	0.5436 (280)	8.1126 (4178)	30	1.0800 (4320)	10.7 ± 0.7
LB 17/35	AP9	3902	11	0.6509 (166)	6.0471 (1542)	80	0.6097 (2439)	9.7 ± 0.8
LB 18/36	AP13	3732	10	0.5522 (127)	5.4217 (1247)	75	0.6097 (2439)	9.2 ± 0.9
Lyoma–Hanle section								
T 92/333	AP16	4225	16	0.5508 (195)	4.7684 (1688)	65	1.0800 (4320)	18.5 ± 1.4
T 93/334	AP18	4200	17	0.6962 (275)	3.7823 (1494)	30	0.5025 (2010)	13.7 ± 1.0
T 94/335	AP7	4200	9	1.0533 (237)	6.4889 (1460)	30	0.5025 (2010)	12.1 ± 1.0
T 95/339	AP5	4200	3	0.9077 (59)	10.8614 (706)	10	1.0800 (4320)	13.4 ± 1.8
T 96/341	AP20	4200	8	0.9804 (150)	10.908 (1669)	95	1.0800 (4320)	14.4 ± 1.2
T 97/343	AP21	4160	6	0.6933 (104)	7.6933 (1154)	90	1.0800 (4320)	14.4 ± 1.5
T 98/345	AP3	4160	7	0.6750 (108)	4.6812 (749)	60	1.0800 (4320)	23.1 ± 2.4
T 99/346	AP1	4200	11	0.8387 (260)	8.4419 (2617)	75	1.0800 (4320)	15.9 ± 1.1
T 100/350	AP19	4160	16	0.5825 (233)	3.0325 (1213)	> 95	0.6097 (2439)	17.4 ± 1.3
T 101/351	AP2	4160	12	0.7615 (198)	4.3346 (1127)	10	0.6097 (2439)	15.9 ± 1.3

ρ_s , Spontaneous fission track density, 10^6 tr/cm²; N_s , Number of spontaneous tracks counted; N_i , Number of induced tracks counted; ρ_i , Induced track density in mica detector; ρ_d , Induced track density in glass dosimeter; $P(\chi^2)$, Probability of obtaining observed χ^2 value for (number of crystals – 1) degrees of freedom, which is quoted nearest to 5%.

The ages were calculated using $T = 1/\lambda_d \ln[1 + G\zeta\lambda_d(\rho_s\rho_d/\rho_i)]$, where λ_d is the total decay constant of U²³⁸ ($=1.55125 \times 10^{-10}$ per year), G is the geometry factor ($= 0.5$, as the spontaneous tracks were counted under 4π conditions), ρ_s is the spontaneous track density, and ζ is the zeta calibration factor (zeta value used $= 296.96 \pm 8.18$ (D. Kumar, unpublished) on Standard Glass Corning 5 (CN5) prepared by Dr J. W. H. Schreurs at Corning Glass Works, Corning, New York, USA).

Table 2. Zircon fission track data of Ladakh batholith

Sample code	Lab code	Elevation (m)	No. of crystals	Track density		$P(\chi^2)$ (%)	Glass dosimeter $\rho_d(N_d)$	Age (Ma)
				Spontaneous $\rho_s(N_s)$	Induced $\rho_i(N_i)$			
LB10/28	Zr 14	5301	09	9.5614 (545)	22.491 (1282)	50	0.6632 (2653)	41.7 ± 2.3
LB12/30	12/30z	4893	04	9.2609 (213)	20.9565 (482)	50	0.6632 (2653)	43.4 ± 3.4
T100/350	Zr 15	4160	02	4.875 (195)	15.1000 (604)	50	0.6632 (2653)	31.7 ± 2.7

from a maximum of 25.3 ± 2.6 Ma to a minimum of 9.2 ± 0.9 Ma over the entire length of the Ladakh batholith under investigation. Oldest fission track apatite ages have been encountered from the highest elevations: 23.1 ± 1.1 Ma from Khardung La (K2, 5440 m) and $25.3 \pm$

2.6 Ma from Chang La (LB10/28, 5301 m). FT apatite reveals a good correlation with elevation and shows younger cooling ages with decreasing elevation (Figure 2 a, b). These ages are 11.8 ± 1.1 Ma at the lowest elevation (NS9/20, 4038 m) in the Khardung La section (Figure 2 a)

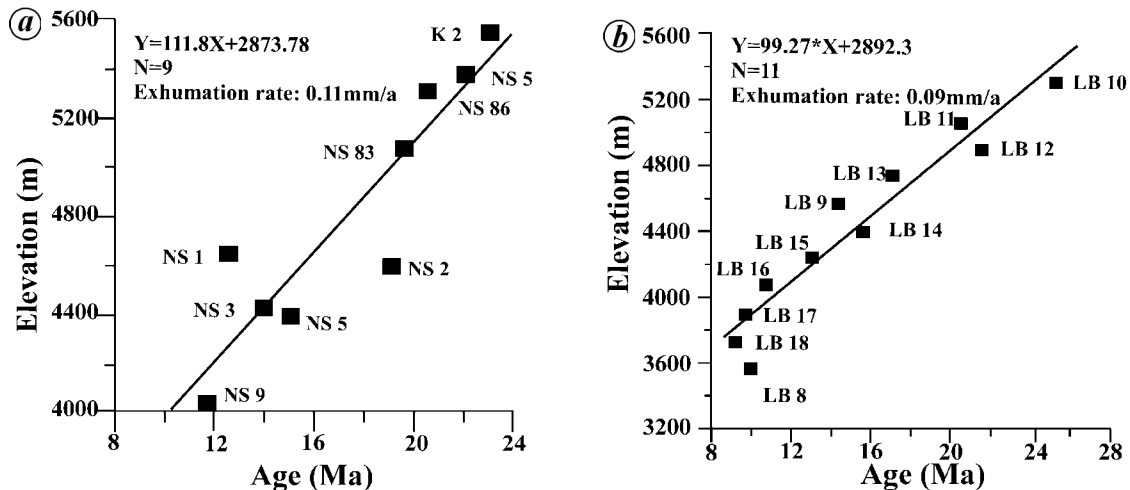


Figure 2. Apatite FT age vs elevation plots of the Ladakh batholith from (a) Leh–Khardung La section and (b) Kharu–Chang La section.

and 9.2 ± 0.9 Ma in the Chang La section (Figure 2b) near Kharu (LB18/36, 3732 m). In the third section, FT apatite ages are clustered between 12.1 ± 0.9 and 18.5 ± 1.4 Ma for samples lying between 4160 and 4225 m, except for sample T98/345, which yields much higher age of 23.1 ± 2.4 Ma. In fact, in this section FT apatite ages do not reveal any significant variation over a distance of more than 170 km almost being at the same elevation.

FT zircon ages of three samples, LB10/28 and LB12/30 from the Chang La section and T100/350 from the Lyoma–Hanle section are 41.7 ± 2.3 , 43.4 ± 3.4 and 31.7 ± 2.7 Ma at 5301, 4893 and 4160 m elevation respectively.

Chemical composition of apatite

The rate of thermal annealing in apatite is also dependent on chemical composition of host apatite crystal, especially the ratio of $(\text{Cl}/\text{Cl} + \text{F})^{26}$ with higher rates of annealing for fluorine-rich apatite relative to chlorine-rich apatite at a given temperature. This compositional effect implies that individual apatite grains from the same sample can display different degrees of thermal annealing even though they have experienced the same thermal history.

To investigate the effects of chlorine and fluorine contents on apatite ages, chemical composition of seven apatite samples from all the three sections was determined. These measurements were made using JEOL JXA-8600M EPMA (Electron Probe Micro Analyzer) with a 15 kV accelerating voltage and 2×10^{-8} A sample current, having a beam size of 1 μm . In each sample, 4–5 apatite grains were analysed to calculate the mean values. The separates from the samples were mounted and polished in the same manner as they were mounted for polishing and irradiation, and taken for the EPMA analysis (Data is available from the authors on request.).

Cl content in samples was found to be much less than F content. These values fall between end-member fluorapatite and Cl content of Durango apatite (Mexico), and are much less than the 0.4 wt% of Cl content of the latter. The $(\text{Cl}/\text{Cl} + \text{F})$ ratio varies from 0.008 to 0.34; hence the chemical composition of apatite appears to have no effects on the annealing properties of fission track, and consequently on the FT ages²⁷.

Discussion

Cooling and exhumation rates

The initial manifestation of the Andean-type margin appeared only in Cenomanian after subduction of the Neo-Tethys oceanic lithosphere beneath the South Asian margin, when the Ladakh batholith pluton was emplaced around 103 to 50 Ma and crystallized at $\sim 750^\circ\text{C}$ in pulses at an approximate depth of 15–20 km. These bodies crystallized between 103 and 101 Ma near Kargil^{15,28} (conventional U–Pb zircon ages), granodiorite to diorite near Leh yielding zircon growths between 60 and 58 Ma^{29,30} (SHRIMP U–Pb zircon ages), granodiorite to granite of 60 ± 10 Ma near Shey¹⁵ (Rb–Sr whole rock isochron age), and a quartz diorite intrusion²⁹ of 49.8 ± 0.8 Ma. High-temperature cooling ages are indicated by $^{40}\text{Ar}/^{39}\text{Ar}$ hornblende and biotite and Rb/Sr biotite ages between 46 and 44 Ma due to either magmatic or tectonic cooling^{15,28,29}. It is, therefore, evident that the FT zircon and apatite ages from the Ladakh batholith reveal its low temperature cooling history.

In apatite and zircon uranium FTs are metastable due to recombination of defects causing fading of tracks and annealing at elevated temperatures. Annealing behaviour of apatite fission tracks and closure temperature for their retention have been estimated by extrapolation of laboratory annealing data to geological time^{1,31}, as well as from

borehole samples of reasonably well-known thermal history, where increasing depth and temperature produce decrease in age^{33,34}. For FT in zircon, annealing experiments³³ and borehole data³⁵ estimate the closure temperature between 200 and 250°C for different cooling rates. Therefore, closure temperatures of FT zircon and apatite are considered to be 220 ± 25 and $110 \pm 10^\circ\text{C}$ respectively. Keeping in mind already published work in NW Himalayas, geothermal gradient of $30^\circ\text{C}/\text{km}$ has been taken in the present work, while mean annual surface temperature of $10 \pm 5^\circ\text{C}$ has been adopted by several workers in the Himalayas⁵ and the Alps^{4,36}.

The exhumation rate of a body can be estimated by:
Exhumation rate = Cooling rate/thermal gradient.

Alternatively, when apatite and/or zircon ages invariably increase with altitude due to the earlier passage of the upper sample below the closure temperature for the retention of tracks, then for limited lateral extent, the difference in elevation divided by the difference in ages provides a direct measurement of exhumation rate^{5,7}. Such values are free from large errors of closure temperatures. This approach is widely used and has also been employed in granitic terrains of Eastern Cordillera of Peru³⁷. This gives the exhumation rate without any assumption of the geothermal gradient and closure temperature.

Considering the apatite FT ages, and the age vs elevation plot (Figure 2) in the two sections, slope of the line gives the exhumation rate, which is 0.1 mm/a for both the Khardung La and Chang La sections during the timespan of 25.3 to 9.2 Ma. Ages are tightly clustered between 17.4 and 12.0 Ma in the Lyoma section, having no significant elevation difference, except one sample having an age of 23.1 Ma.

Datable zircons by the FT method during the course of this work could be obtained only from three samples; LB10/28, LB12/30 from the Chang La section and T100/350 from the Lyoma–Hanle. However, statistical quality of the data is not good due to nonavailability of large number of crystals. Their ages came out to be 41.7 ± 2.3 , 43.4 ± 3.4 and 31.7 ± 2.7 Ma from two sections from west to the east respectively. These samples are located at 5301, 4893 and 4160 m respectively. Considerable younging of the FT zircon ages is noticeable towards east, though it could not be confirmed due to lack of more datasets. Considering these ages, cooling rates for these samples are 6.71, 5.05 and $7.67^\circ\text{C}/\text{Ma}$ with exhumation rates of 0.2, 0.2 and 0.3 mm/a respectively, with mean exhumation rate of 0.2 mm/a between the corresponding zircon and apatite ages.

FT apatite ages⁶, obtained on four granitoid samples of the Kargil igneous complex in the extreme west, range from 13.2 ± 2.4 to 24.7 ± 2.5 Ma with track length of $16.6 \pm 0.2 \mu\text{m}$ and SD of $1 \mu\text{m}$. These have been interpreted to be indicative of rapid cooling.

In comparison to the FT dataset from the Ladakh batholith generated for in this work, the FT apatite age of 5 ± 1 Ma has been obtained¹² from one sample at Chumathang with mean track length of $14.73 \pm 0.14 \mu\text{m}$. This has been interpreted as diagnostic of rapid cooling through partial annealing zone of $60\text{--}110^\circ\text{C}$ due to longer residence period of the batholith at greater depth as a result of its local overthrusting by the Indus molasses deposits¹². On the other hand, our data give a range of AFT ages from 25.3 to 9.2 Ma and are indicative of slow and simple cooling history.

However, FT apatite ages of 28 ± 3 and 29 ± 2 Ma from the Ladakh batholith from Upshi¹⁴ are much older than 10.0 ± 0.8 Ma obtained in this work around Kharu, which is nearest to this locality. The FT apatite ages from two sedimentary sequences in the immediate vicinity of the Ladakh batholith, i.e. the Nimmu Formation are 14 ± 3 Ma and 12 Ma from a boulder¹⁴ in Choksti conglomerate from Zanskar gorge. From these ages and extrapolation with the illite crystallinity, it was deciphered that the termination of sediment accumulation in the Indus Valley took place in early Miocene¹⁴, with the initiation of a palaeo-Indus river in this area < 26 Ma. Interestingly, considering that the samples at the highest elevations of 5300 to 5400 m from the Ladakh batholith had crossed the $110 \pm 10^\circ\text{C}$ geotherm (> 3.5 km depth) between 23 and 25 Ma, one would expect that the overlying batholith column at the surface, available for erosion, would have shown FT apatite age of $\sim 24\text{--}26$ Ma, considering the average exhumation rate of 0.1 mm/yr. It is, therefore, evident from our data as well, that the Ladakh batholith possibly was first exposed to the surface between 24 and 26 Ma and was drained-off by the palaeo-Indus river around that time on its southern slopes, as has been deciphered earlier¹⁴.

Two FT zircon ages⁶ of 41.4 ± 2.2 and 45.2 ± 3.1 Ma from the Kargil body and the ages obtained in this work are in agreement. From this similarity, it can be inferred that the whole batholith from west to east in the Ladakh range has crossed the $220 \pm 10^\circ\text{C}$ geotherm between 42 and 45 Ma.

FT zircon age of 40.5 ± 2.1 Ma from sandstone of the Chultze Molasse appears to be derived from a single source as erosional product, probably from the emplaced North Himalayan nappe stack much to the south¹². Instead, our zircon FT data clearly reveal that part of the Ladakh batholith crossed the $220 \pm 25^\circ\text{C}$ isotherm between 43 and 32 Ma in the region between Upshi and Lyoma, thus becoming a strong provenance for the Indus sediments during Oligocene.

Summary

Following the closure of the Neo-Tethys and subsequent continental collision of India–Asia blocks ~ 55 Ma^{15,29}, major pulse of uplift and erosion had occurred in Ladakh.

The Ladakh batholith, after its crystallization^{15,30} at ~60 Ma, has undergone normal magmatic cooling at a rate of about 30°C/Ma till 45–46 Ma, as suggested by Rb–Sr and K–Ar biotite cooling ages. As a consequence of the India–Asia collision, cooling and exhumation have been relatively fast in the span of 45–46 to 42–43 Ma (FT zircon cooling age). After 42–43 Ma, the batholith has cooled and exhumed at a slow rate. This is evidenced from zircon FT ages of 42–43 Ma and maximum apatite age of 25.4 Ma. Between this timespan, the batholith has cooled down @ 7.0°C/Ma and exhumed at a rate of 0.2 mm/a. From 25.4 Ma to the minimum apatite FT age of 9.2 Ma, the Ladakh batholith has exhumed at an average rate of 0.1 mm/a. After the minimum FT apatite age of the dated sample at 9.2 Ma to the Present, the batholith again cooled and exhumed somewhat rapidly with a rate of 0.3 mm/a, which is almost three times the exhumation from 25.4 to 9.2 Ma. These patterns of low-temperature cooling and exhumation in the Trans-Himalayan Ladakh batholith have incurred in relatively older times and are much slower than the contrasting patterns of the Higher Himalayan Metamorphic belt further south.

1. Naeser, C. W., Fission track dating and geologic annealing of fission tracks. In *Lectures in Isotope Geology* (eds Jager, E. and Hunziker, J. C.), Springer-Verlag, Heidelberg, 1979, pp. 154–169.
2. Kohn, B. P., Shagam, R., Banks, P. O. and Burkley, E. A., Mesozoic–Pleistocene fission track ages on rocks of the Venezuelan Andes and their tectonic implications. *Mem. Geol. Soc. Am.*, 1984, **162**, 365–384.
3. Fitzgerald, P. G., Sandiford, M., Barrett, P. J. and Gleadow, A. J. W., Asymmetric extension associated with uplift and subsidence in the Transantarctic Mountains and Ross Embayment. *Earth Planet. Sci. Lett.*, 1986, **81**, 67–78.
4. Wagner, G. A., Reimer, M. and Jager, E., Cooling ages derived by apatite fission track, mica Rb/Sr and K/Ar dating, the uplift and cooling history of the Central Alps. *Mem. Ist. Geol. Mineral. Univ. Padova*, 1977, 30–38.
5. Kumar, A., Lal, N., Jain, A. K. and Sorkhabi, R. B., Late Cenozoic–Quaternary thermo-tectonic history of Higher Himalayan Crystallines (HHC) in Kishtwar–Padar–Zanskar region, NW Himalaya: Evidences from fission track ages. *J. Geol. Soc. India*, 1995, **45**, 375–391.
6. Sorkhabi, R. B., Jain, A. K., Nishimura, S., Itaya, T., Lal, N., Manickavasagam, R. M. and Tagami, T., New age constraints on the cooling and unroofing history of the Trans Himalayan Ladakh batholith (Kargil area), N. W. India. *Proc. Indian Acad. Sci. (Earth Planet. Sci.)*, 1994, **103**, 83–97.
7. Sorkhabi, R. B., Stump, E., Foland, K. A. and Jain, A. K., Fission track and ⁴⁰Ar/³⁹Ar evidence for episodic denudation of the Gangotri granites in the Garhwal Himalaya, India. *Tectonophysics*, 1996, **260**, 187–199.
8. Sorkhabi, R. B., Jain, A. K., Nishimura, S., Itaya, T., Fukui, S., Lal, N. and Kumar, A., Cooling age record of domal uplift in the core of the Higher Himalayan Crystallines (HHC), Southwest Zanskar, India. *Proc. Indian Acad. Sci. (Earth Planet. Sci.)*, 1997, **106**, 169–179.
9. Sorkhabi, R. B., Stump, E., Foland, K. A. and Jain, A. K., Tectonic and cooling history of the Garhwal Higher Himalaya (Bhagirathi valley): constraining from thermochronological data. In *Geodynamics of the NW-Himalaya* (eds Jain, A. K. and Manickavasagam, R. M.), Gondwana Res. Group Mem. No. 6, 1999, pp. 217–235.
10. Lal, N., Mehta, Y. P., Kumar, D., Kumar, A. and Jain, A. K., Cooling and exhumation history of the Mandi Granite and adjoining tectonic units, Himachal Pradesh, and estimation of closure temperature from external surface of zircon. In *Geodynamics of the NW-Himalaya* (eds Jain, A. K. and Manickavasagam, R. M.), Gondwana Res. Group Mem. No. 6, 1999, pp. 207–216.
11. Jain, A. K., Kumar, D., Singh, S., Kumar, A. and Lal, N., Timing, quantification and tectonic modeling of Pliocene Quaternary movements in the NW Himalaya: Evidences from fission track dating. *Earth Planet. Sci. Lett.*, 2000, **179**, 437–451.
12. Schlup, M., Carter, A., Cosca, M. and Steck, A., Exhumation history of eastern Ladakh revealed by ⁴⁰Ar/³⁹Ar and fission track ages: The Indus river–Tso Morari transect, NW Himalaya. *J. Geol. Soc. London*, 2003, **160**, 385–399.
13. Theide, R. C., Bookhagen, B., Arrowsmith, J. R., Sobel, E. R. and Strecker, M. R., Climatic control on rapid exhumation along the Southern Himalayan Front. *Earth Planet. Sci. Lett.*, 2004, **222**, 791–806.
14. Sinclair, H. D. and Jaffey, N., Sedimentology of the Indus Group, Ladakh, northern India: Implications for the timing of initiation of paleo-Indus River. *J. Geol. Soc. London*, 2001, **158**, 151–162.
15. Honegger, K., Dietrich, V., Frank, W., Gansser, A., Thoni, M. and Trommsdorff, V., Magmatism and metamorphism in the Ladakh Himalaya (the Indus–Tsangpo suture zone). *Earth Planet. Sci. Lett.*, 1982, **60**, 253–292.
16. Thakur, V. C., *Geology of the Western Himalaya*, Pergamon Press, Oxford, 1993, p. 355.
17. Jain, A. K., Singh, Sandeep and Manickavasagam, R. M., *Himalayan Collision Tectonics*, Gondwana Research Group Memoir No. 7, 2002, p. 114.
18. Sharma, K. K. and Choubey, V. M., Petrology, geochemistry and geochronology of the southern margin of the Ladakh batholith between Upshi and Chumathang. In *Geology of Indus Suture Zone of Ladakh* (eds Thakur, V. C. and Sharma, K. K.), Wadia Institute of Himalayan Geology, Dehradun, 1983, pp. 41–60.
19. Raz, U. and Honneger, K., Magmatic and tectonic evolution of the Ladakh block from field studies. *Tectonophysics*, 1989, **161**, 107–118.
20. Rolland, Y., Pecher, A. and Picard, C., Middle Cretaceous back-arc formation and arc evolution along the Asian margin: The Shyok Suture Zone in Northern Ladakh (NW Himalaya). *Tectonophysics*, 2000, **325**, 145–173.
21. Gleadow, A. J. W. and Duddy, I. R., A natural long track annealing experiment for apatite. *Nucl. Tracks*, 1981, **5**, 169–174.
22. Tagami, T., Lal, N., Sorkhabi, R. B., Ito, H. and Nishimura, S., Fission track dating using external detector method: A laboratory procedure. *Mem. Fac. Sci., Kyoto Univ., Ser. Geol. Mineral.*, 1988, **53**, 1–30.
23. Hurford, A. J. and Green, P. F., A users' guide to fission track dating calibration. *Earth Planet. Sci. Lett.*, 1982, **59**, 343–346.
24. Hurford, A. J. and Green, P. F., The zeta age calibration of fission track dating. *Isot. Geosci.*, 1983, **1**, 285–317.
25. Hurford, A. J., Standardization of fission track dating calibration: recommendation by the fission track geochronology. *Chem. Geol.*, 1990, **80**, 171–178.
26. Green, P. F., Duddy, I. R., Gleadow, A. J. W. and Lovering, J. F., Apatite fission track analysis as a paleotemperature indicator for hydrocarbon exploration. In *Thermal History of Sedimentary Basins* (eds Naeser, N. D. and McCullon, Th.), Springer-Verlag, New York, 1989, pp. 181–195.
27. Young, E. J., Myers, A. T., Munson, E. L., Conklin, N. M., Mineralogy and geochemistry of fluorapatite from Cerro Mercado, Durango, Mexico. *U.S. Geol. Surv. Prof. Pap.* 650, 1969, **D84**.
28. Scharer, U., Hamet, J. and Allegre, C. J., The Trans Himalaya (Gangdese) plutonism in the Ladakh region: a U–Pb and Rb–Sr study. *Earth Planet. Sci. Lett.*, 1984, **67**, 327–339.

RESEARCH ARTICLES

29. Weinberg, R. F. and Dunlap, J., Growth and deformation of the Ladakh batholith, Northwest Himalayas: Implications for timing of continental collision and origin of calc-alkaline batholiths. *J. Geol.*, 2000, **108**, 303–320.
30. Singh, S., Kumar, R., Barley, M. E. and Jain, A. K., SHRIMP U–Pb ages and depth of emplacement of Ladakh Batholith, eastern Ladakh, India. *J. Asian Earth Sci.*, 2007, doi:10.1016/j.jseas.2006.12.003.
31. Nagpaul K. K., Mehta, P. P. and Gupta, M. L., Annealing studies on radiation damages in biotite, apatite and sphene and corrections to fission track ages. *Pure Appl. Geophys.*, 1974, **112**, 131–139.
32. Fleischer, R. L., Price, P. B. and Walker, R. M., Effects of temperature, pressure and ionization on the formation and stability of fission tracks in minerals and glasses. *J. Geophys. Res.*, 1965, **70**, 1497–1503.
33. Krishnaswami, S., Lal, D., Prabhu, N. and McDougall, D., Characteristics of fission tracks in zircon: application to geochronology and cosmology. *Earth Planet. Sci. Lett.*, 1974, **22**, 51–59.
34. Tagami, T., Ito, H. and Nishimura, S., Thermal annealing characteristics of spontaneous fission tracks in zircon. *Chem. Geol.*, 1990, **80**, 159–169.
35. Zaun, P. E. and Wagner, G. A., Fission track stability in zircons under geological conditions, *Nucl. Tracks*, 1985, **10**, 303–307.
36. Hurford, A. J., Cooling and uplift patterns in Leptonite Alps, South Central Switzerland and age of vertical movement on the Insubric fault line. *Contrib. Mineral. Petrol.*, 1986, **92**, 413–427.
37. Laubacher, G. and Naeser, C. W., Fission-track dating of granitic rocks from the Eastern Cordillera of Peru: Evidences for Late Jurassic and Cenozoic cooling. *J. Geol. Soc. London*, 1994, **151**, 473–483.

ACKNOWLEDGEMENTS. We are grateful to the Department of Science and Technology, New Delhi for providing funds under the research project HIMPROBE (A.K.J., N.L., S.S.), and making it possible to undertake the field work. Financial assistance from the Council of Scientific and Industrial Research, New Delhi to R.K. is acknowledged. Prof. Kailash Chandra and Dr T. K. Ghosh, Institute Instrumentation Center, IIT Roorkee, are acknowledged for providing the EPMA facilities. Constructive comments by the anonymous reviewer have improved the manuscript.

Received 16 January 2006; revised accepted 15 October 2006
